FULL PAPER

Dalton
www.rsc.org/dalton

Synthesis and study of new binuclear compounds containing bridging (μ-CN)B(C_6F_5)$_3$ and (μ-NC)B(C_6F_5)$_3$ systems

Ino C. Vei, Sofia I. Pascu, Malcolm L. H. Green,* Jennifer C. Green, Richard E. Schilling, Grant D. W. Anderson and Leigh H. Rees
Inorganic Chemistry Laboratory, South Parks Road, Oxford, UK OX1 3QR

Received 24th February 2003, Accepted 2nd May 2003
First published as an Advance Article on the web 23rd May 2003

The new compounds [K(18-crown-6)][SCNB(C_6F_5)$_3$] (**1**), [K(18-crown-6)][(C_6F_5)$_3$B(μ-NC)B(C_6F_5)$_3$] (**2**), [K(18-crown-6)][NCB(C_6F_5)$_3$] (**3**), [Me_3Si(μ-NC)B(C_6F_5)$_3$] (**4**) and [Hg{(μ-CN)B(C_6F_5)$_3$}$_2$] (**5**) have been synthesised. Reaction between [IrCl(PPh_3)$_2$(CO)] and one equivalent of **4** gives [Ir{(μ-NC)B(C_6F_5)$_3$}(PPh_3)$_2$CO] (**6**). Similarly, the reaction between [Fe(η-C_5H_5)(CO)$_2$Cl] and **4** gives [Fe{(μ-NC)B(C_6F_5)$_3$}(η-C_5H_5)(CO)$_2$] (**7a**). The NMR-scale reaction between [Fe(η-C_5H_5)(CO)$_2$CN] and B(C_6F_5)$_3$ gives the isomer [Fe{(μ-CN)B(C_6F_5)$_3$}(η-C_5H_5)(CO)$_2$] (**7b**). In the compounds **3**, **4**, **6** and **7a** the anion [NCB(C_6F_5)$_3$]$^-$ is coordinated to the metal through the nitrogen. Complexes **1**, **2** and **7b** incorporate a (μ-CN)B unit. The compounds containing the isomeric bridging (μ-CN)B or (μ-NC)B systems have been investigated by ^{11}B{^{1}H} NMR spectroscopy and by DFT calculations. The ^{11}B{^{1}H} NMR spectra enable distinction between the isomers. The single-crystal X-ray structures of **1**, **3** and **7a** have been determined.

Introduction

Compounds incorporating the weakly coordinating anion [(C_6F_5)$_3$B(μ-CN)B(C_6F_5)$_3$]$^-$ together with cationic metallocenes have recently been reported by Bochmann and co-workers to give active homogenous catalysts for olefin polymerisation.[1,2] The compound [Zr{(μ-NC)B(C_6F_5)$_3$}Me(Cp″)$_2$], where Cp″ = 1,3-C_5H_3($SiMe_3$)$_2$, containing the anionic isonitrile ligand [NCB(C_6F_5)$_3$]$^-$ has also been reported.[2] The complexes [$NHMe_2Ph$]$_2$[Ni{(μ-CN)B(C_6F_5)$_3$}$_4$] and [Ph_3C]$_2$[Ni{(μ-CN)-B(C_6F_5)$_3$}$_4$] are active as co-catalysts towards olefin polymerisation.[2]

Earlier we have described some coordination chemistry of B(C_6F_5)$_3$ and of the anionic ligand [HOB(C_6F_5)$_3$]$^-$. [3–8] Here we describe the potassium salts of the new anions [SCNB(C_6F_5)$_3$]$^-$ and [NCB(C_6F_5)$_3$]$^-$, the adducts of B(C_6F_5)$_3$ with Me_3SiCN and Hg(CN)$_2$, and the organometallic compounds [Ir{(μ-NC)-B(C_6F_5)$_3$}(PPh_3)$_2$(CO)], [Fe{NCB(C_6F_5)$_3$}(η-C_5H_5)(CO)$_2$] and [Fe{(μ-CN)B(C_6F_5)$_3$}(η-C_5H_5)(CO)$_2$].

The neutral isonitrile adducts [RNCBC$_6F_5$)$_3$] [9] and nitrile adducts [RCNB(C_6F_5)$_3$] [9–11] (R = alkyl, aryl)) have been reported previously. They contain the units E_1NCB or E_1CNB, respectively, where E_1 = alkyl, aryl, hydrocarbyl. The organic compounds E_1NC and E_1CN are commonly described as isonitriles (isocyano) or nitriles (cyano), respectively. However when we consider the bridging systems E_1(μ-CN)E_2 or E_1(μ-NC)E_2 where E_1 and E_2 are not carbon bonding groups the use of the terms "nitrile" or "isonitrile" can lead to confusion. Of course, for E_1(μ-CN)E_2, if E_1 is a hydrocarbyl group and E_2 is, for example, a metal, then description as "an organo nitrile ligand to the metal" would be appropriate. There are in fact only a few two-atom bridging (μ-AB) ligands which can adopt both E_1(μ-AB)E_2 and E_1(μ-BA)E_2 structures with a similar facility, and we are not aware of a systematic notation for isomers in the class E_1(μ-CN)E_2 and E_1(μ-NC)E_2. Therefore, we will describe the compounds containing the units E_1(μ-CN)E_2 or E_1((μ-NC)E_2 simply by defining the elements E_1 and E_2 in each case. In this work the E_2 atom is boron.

DOI: 10.1039/b302163g

Results and discussion

Syntheses

The reaction between KSCN and B(C_6F_3)$_3$ in the presence of 18-crown-6 ether, in toluene, gave [K(18-crown-6)][SCNB-(C_6F_5)$_3$] (**1**), and the reaction between 18-crown-6 ether, KCN and B(C_6F_3)$_3$ (in a 1 : 1 : 1 ratio or a 1 : 1 : 2 ratio) in toluene gave [K(18-crown-6)][(C_6F_5)$_3$B(μ-NC)B(C_6F_5)$_3$] (**2**) instead of the expected [K(18-crown-6)][NCB(C_6F_5)$_3$] (**3**). The anion [(C_6F_5)$_3$B(μ-CN)B(C_6F_5)$_3$]$^-$ has been reported earlier as the [Ph_3C]$^+$ salt.[1,2] Alternative routes for the synthesis of **3** *via* treatment of [K(18-crown-6)][CN] with B(C_6F_5)$_3$ were explored. The reaction was performed in toluene, CH_2Cl_2, THF and CH_3CN, but gave only [K(18-crown-6)][(C_6F_5)$_3$B(μ-CN)-B(C_6F_5)$_3$] (**2**) and not **3**. An NMR scale reaction between Me_3SiCN and B(C_6F_5)$_3$ in C_6D_6 or CD_2Cl_2 gave a clean spectrum consistent with the formation of [(Me_3Si)(μ-NC)-B(C_6F_5)$_3$] (**4**). This was surprising, since the product expected was [(Me_3Si)(μ-CN)B(C_6F_5)$_3$]. However, we note that rapid equilibrium between R_3SiCN and R_3SiNC is well established.[12–15] A larger scale synthesis in CD_2Cl_2 led to the formation of **4** in 77% yield. Since a facile cleavage of the anion [NCB(C_6F_5)$_3$]$^-$ from the adduct **4** was expected, the reaction of this adduct with KCl (in presence of 18-crown-6 ether) was carried out in toluene and the desired compound [K(18-crown-6)][NCB(C_6F_5)$_3$]$^-$ (**3**) was isolated in 73% yield.

Another attempt to synthesise the isonitrile anion [CNB-(C_6F_5)$_3$]$^-$ was made by cleavage, using potassium metal, of the adduct [Hg{(μ-CN)B(C_6F_5)$_3$}$_2$] (**5**). The new compound **5** was synthesised by addition of [Hg(CN)$_2$] to B(C_6F_5)$_3$ in CH_2Cl_2. The adduct **5** is decomposed by water to give, *inter alia*, the known adduct [H_2OB(C_6F_5)$_3$].[3] Attempts to form either H[CNB(C_6F_5)$_3$] or H[NCB(C_6F_5)$_3$] by treatment of **5** with H_2S were unsuccessful. The reduction of the Hg(II) adduct **5** with potassium metal in the presence of 18-crown-6 ether was carried out in toluene at 90 °C. The nitrile compound [K(18-crown-6)][NCB(C_6F_5)$_3$] (**3**) was isolated in moderate yield, as white crystals. There was no evidence for the isomer [K(18-crown-6)][CNB(C_6F_5)$_3$].

Reaction between [IrCl(PPh_3)$_2$(CO)] and [Me_3Si(μ-NC)-B(C_6F_5)$_3$] (**4**) in CH_2Cl_2 gave an initial pale-yellow mixture which changed to a bright yellow after 2 h. Bright-yellow crystals of the complex [Ir{(μ-NC)B(C_6F_5)$_3$}(PPh_3)$_2$(CO)] (**6**) were obtained by crystallisation from CH_2Cl_2. Treatment of [Fe(η-C_5H_5)(CO)$_2$Cl] with one equivalent of **4** in pentane as room temperature formed red crystals of [Fe{(μ-NC)-B(C_6F_5)$_3$}(η-C_5H_5)(CO)$_2$] (**7a**). The isomer [Fe{(μ-CN)-B(C_6F_5)$_3$}(η-C_5H_5)(CO)$_2$] (**7b**) could be prepared in solution by the treatment of [Fe(η-C_5H_5)(CO)$_2$(CN)] with B(C_6F_5)$_3$ in C_6D_6 and has been characterised only by NMR data in solution.

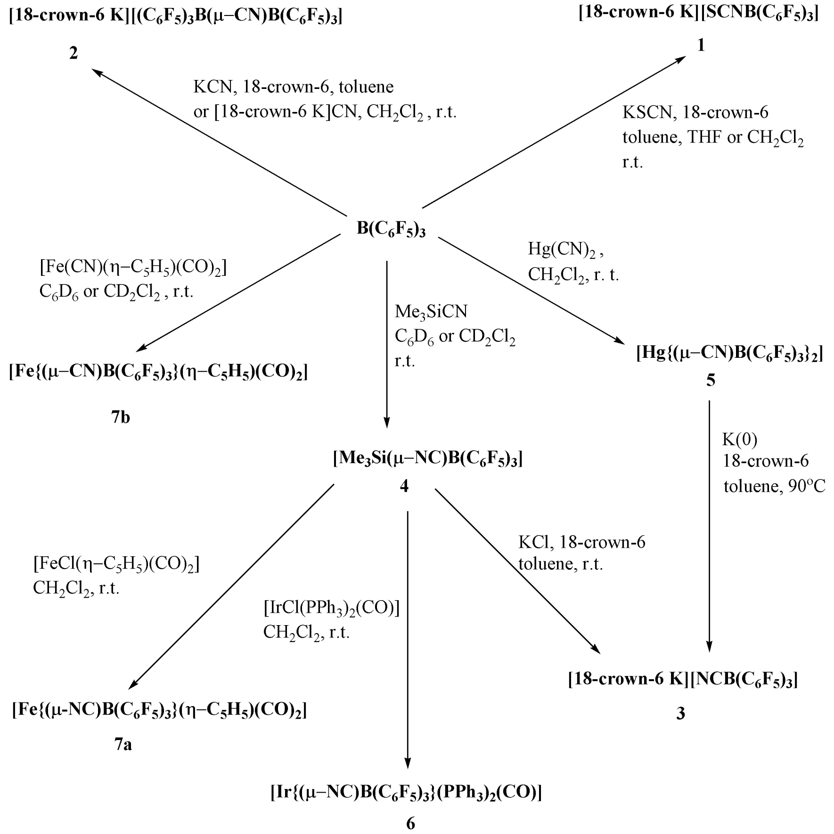

Scheme 1 Formation of compounds **1**–**6**, **7a** and **7b**.

Scheme 1 shows the syntheses of compounds **1**–**6**, **7a** and **7b**, which are highly air- and moisture-sensitive. The new compounds **1**–**7a**, **7b** have been characterised by microanalysis and by infrared and NMR spectroscopy and the data are given in the experimental sections or Tables 1 and 2 and are discussed below. The crystal structures of **1**, **3** and **7a** have been determined.

Spectroscopic studies

The ^{11}B NMR spectra are particularly diagnostic. The ^{11}B resonances differ markedly between three-coordinate borane $B(C_6F_5)_3$ and the four-coordinate boron found in the Lewis acid–base adducts [(Donor)$B(C_6F_5)_3$] for which the ^{11}B resonance is shifted to lower frequency with respect to $B(C_6F_5)_3$ by more than 50 ppm.[3–7, 16]

The ^{11}B data for a number of known compounds and for compounds described in this work are listed in Table 2. The data show that when boron is directly bonded to nitrogen, as in $E_1(\mu\text{-}CN)B$, the $^{11}B\{^1H\}$ resonance is *broad* and occurs in the range δ −9.0 to −13.0 ppm. When boron is directly attached to carbon, as in $E_1(\mu\text{-}NC)B$, the $^{11}B\{^1H\}$ resonance is *sharp* and occurs in the range δ −20.0 to −23.0 ppm. On this basis the structures of the isomeric compounds **7a** and **7b** can be assigned as shown in Table 2.

The ^{19}F NMR spectra of all the new compounds show resonances broadly similar to those of $B(C_6F_5)_3$ but shifted to lower frequency. The *para* – fluorine resonances were found to be the most sensitive of the aromatic fluorine shifts. The ^{19}F NMR data for derivatives of nitrile- or isonitrile-borates, (containing the RCNB and RNCB units) have been found to be distinct from the free borane, however they do not permit a reliable distinction between two isomers such as **7a** and **7b**.

The IR spectra of compounds **1**–**6** and **7a** in Table 1 show sharp bands in the region 2146–2284 cm^{-1} which can be assigned to the ν_{CN} or ν_{NC} stretching frequencies. As previously shown,[9] the coordination of $B(C_6F_5)_3$ to a E_1CN^- group causes a significant band shift to higher wavenumbers. Thus the IR spectrum of the complex [$Me_3Si(\mu\text{-}NC)B(C_6F_5)_3$] (**4**) shows a band at 2255 cm^{-1} compared to 2190 cm^{-1} for Me_3SiCN. The corresponding wavenumber for [$Fe(\eta\text{-}C_5H_5)(CO)_2CN$] is 2114 cm^{-1} and for [$Fe\{(\mu\text{-}NCB(C_6F_5)_3\}(\eta\text{-}C_5H_5)(CO)_2$] (**7a**) it is 2252 cm^{-1}.

X-Ray crystallography

The crystal structures of compounds **1**, **3** and **7a** have been determined. Selected molecular parameters are given in Table 3 and Table 4 presents the X-ray crystallographic data. Single crystals of **1** suitable for the X-ray structure analysis were grown by diffusion of pentane into a dichloromethane solution. An ORTEP of **1** is presented in Fig. 1. The X-ray crystal structure analysis of **1** confirms that only one equivalent of 18-crown-6 ether is present in the asymmetric unit and

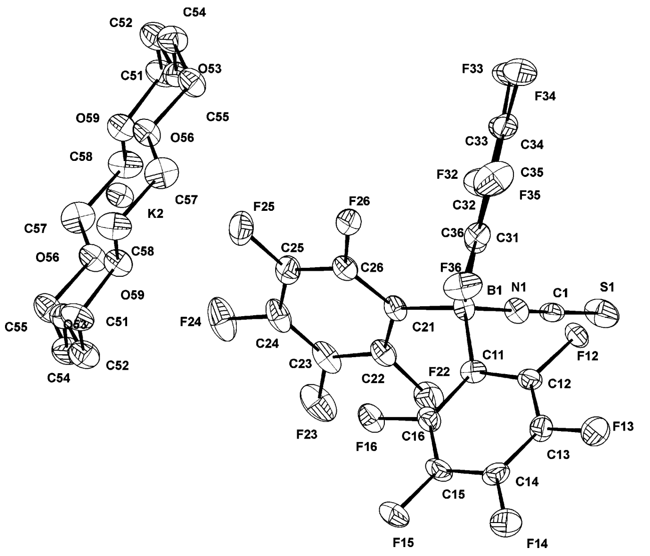

Fig. 1 ORTEP of [K(18-crown-6)][$SCNB(C_6F_5)_3$] (**1**).

Table 1 IR (KBr disks, ν in cm^{-1}) and NMR data (C_6D_6, δ in ppm) at room temperature

Compound	IR	^{1}H	^{11}B{^{1}H}	^{19}F-*ortho* (d, 2F, $^2J_{F-F}$ ≈20 Hz)	^{19}F-*para* (br, 1F)	^{19}F-*meta* (br, 2F)
$B(C_6F_5)_3$			58	−128.8	−144.6	−161.5
[K(18-crown-6)K][SCNB(C_6F_5)$_3$] **1**	2146 (ν_{CN})	3.70 (s)	−12.4	−134.7	−160.5	−165.7
[K(18-crown-6)][(C_6F_5)$_3$B(μ-NC)B(C_6F_5)$_3$] **2**	2294.8; 2295.3 (ν_{CN})	3.63 (s)	−12.1; −21.9	−134.6; −135.7	−161.3, −161.4	−168.0, −168.4
[K(18-crown-6)][NCB(C_6F_5)$_3$] **3**	2212 (ν_{CN})	3.54 (s)	−22.5	−132.6	−160.5	−165.8
[Me_3Si(μ-NC)B(C_6F_5)$_3$] **4**	2256 (ν_{CN})	−0.30 (s)	−21.7	−133.7	−155.2	−163.2
[Hg{(μ-CN)B(C_6F_5)$_3$}$_2$] **5**	2284 (ν_{CN})		−10.7	−134.4	−156.7	−164.3
[Ir{(μ-NC)B(C_6F_5)$_3$}(PPh_3)$_2$(CO)] **6**[a]	2232 (ν_{CN}) 2012 ($\nu_{CO\text{-}sym}$) 1962 ($\nu_{CO\text{-}asym}$)	7.38 (m, 6H) 7.56 (m, 4H)	−22.8	−132.16	−159.8	−164.8
[Fe{(μ-NC)B(C_6F_5)$_3$}(η-C_5H_5)(CO)$_2$] **7a**	2252 (ν_{CN}) 2076 ($\nu_{CO\text{-}sym}$) 2032 ($\nu_{CO\text{-}asym}$)	5.15 (s)	−22.4	−134.0	−158.6	−164.7
[Fe{(μ-CN)B(C_6F_5)$_3$}(η-C_5H_5)(CO)$_2$] **7b**	–	5.28 (s)	−12.0	−135.6	−159.3	−169.5

[a] ^{31}P{^{1}H} NMR (C_6D_6) at 25 °C: δ 22.9 (s).

Table 2 Comparative ^{11}B{^{1}H} NMR data. ^{11}B{^{1}H}NMR line shape is described here as *sharp* if $\nu_{1/2}$ is <15 ± 1 Hz, and as *broad* if $\nu_{1/2}$ is >300 ± 10 Hz

Compound	δ ^{11}B{^{1}H}	Line shape	Assignment	Ref.
^{a}[Ph_3C][Pd{(μ-CN)B(C_6F_5)$_3$}$_4$]	−12.8	–	N–B	1
^{b}(MeCN)B(C_6F_5)$_3$	−10.3	Broad	N–B	3
^{b}[(*p*-$NO_2C_6H_4CN$)B(C_6F_5)$_3$]	−9.6	Broad	N–B	3
^{b}[(*p*-MeC_6H_4CN)B(C_6F_5)$_3$]	−10.2	Broad	N–B	3
^{b}[Hg{(μ-CN)B(C_6F_5)$_3$}$_2$] **5**	−10.7	Broad	N–B	This work
^{b}[Fe{(μ-CN)B(C_6F_5)$_3$}(η-C_5H_5)(CO)$_2$] **7b**	−12.0	Broad	N–C	This work
^{b}[K(18-crown-6)][(C_6F_5)$_3$B(μ-NC)B(C_6F_5)$_3$] **2**	−12.1	Broad	N–B	This work
	−21.9	Sharp	C–B	
^{c}[Ph_3C][(C_6F_5)$_3$B(μ-NC)B(C_6F_5)$_3$]	−11.9	–	N–B	2
	−21.6		C–B	
^{b}[(^{t}BuNC)B(C_6F_5)$_3$]	−21.8	Sharp	C–B	3
^{b}[(Me_3C–CH_2–CMe_2–NC)B(C_6F_5)$_3$]	−21.7	Sharp	C–B	3
^{b}[(2,6-$Me_2C_6H_3$)NCB(C_6F_5)$_3$]	−21.0	Sharp		
^{a}[Zr{(μ-NC)B(C_6F_5)$_3$}Me(Cp″)$_2$]^d	−19.6	–	C–B	2
^{b}[K(18-crown-6)][NCB(C_6F_5)$_3$] **3**	−22.5	Sharp	C–B	This work
^{b}[Me_3SiB(μ-NC)B(C_6F_5)$_3$] **4**	−21.7	Sharp	C–B	This work
^{b}[Ir{(μ-NC)B(C_6F_5)$_3$}(PPh_3)$_2$(CO)] **6**	−22.8	Sharp	C–B	This work
^{b}[Fe{(μ-NC)B(C_6F_5)$_3$}(η-C_5H_5)(CO)$_2$] **7a**	−22.4	Sharp	C–B	This work

NMR data in ^{a} CD_2Cl_2, ^{b} C_6D_6, ^{c} $CDCl_3$. ^{d} Cp″ = 1,3-$C_5H_3(SiMe_3)_2$.

the thiocyanate group is connected by a B(1)–N(1) bond (1.531(3) Å). Noteworthy, this bond is significantly shorter than the corresponding boron–nitrogen distances found in [Ph_3C][(C_6F_5)$_3$B(μ-CN)B(C_6F_5)$_3$]$^-$ (1.593(2) Å), [Ph_3C]$_2$[Ni{(μ-CN)-B(C_6F_5)$_3$}$_4$] (1.574(2) Å), [$HNMe_2Ph$]$_2$[Ni{(μ-CN)B(C_6F_5)$_3$}$_4$] (1.582(3) and 1.578(3) Å) and [Ph_3C]$_2$[Pd{(μ-CN)B(C_6F_5)$_3$}$_4$] (1.577(3) and 1.571(3) Å).[1,2] In **1**, the C(1)–N(1) bond is 1.180(3) Å, somewhat longer that those found for several neutral RCNB(C_6F_5)$_3$ adducts (1.124(3) for R = Me and 1.135(3) for R = *p*-$NO_2C_6H_4$),[9] or for the anion [(C_6F_5)$_3$-B(μ-CN)B(C_6F_5)$_3$]$^-$ (1.144(2) Å). [1,2] The C(1)–S(1) distance is 1.598(2) Å and the N(1)–C(1)–S(2) angle is close to linear (178.3(2)°). The coordination geometry about the boron centre is distorted tetrahedral, with N–B–C angles 108.03(18), 106.35(16)° and 106.89(17)° and the C–B–C angles measuring 112.02(16)° (C(11)-B(1)–C(31)), 112.12(16)° (C(11)–B(1)–C(21)) and 112.86(19)° (C(21)–B(1)–C(31)), and the mean B–C(aromatic) distance is *ca.* 1.650 Å. No solvent molecules are present and the closest intermolecular contact is 2.892(13) Å between K(2) and F(25) in an adjacent molecule in which the C(25)–F(25)–K(2) angle is 136.35(16)°. The cation is bound to B(C_6F_5)$_3$ *via* fluorine bridges, to form a chain-like supramolecular structure, as shown in Fig. 2. This structure accounts for the exceptional stability of **1** towards the attack of nucleophiles such as H_2O or PMe_3.

X-Ray diffraction methods alone cannot reliably distinguish between carbon and nitrogen in the systems E_1(μ-CN)E_2 and E_1(μ-NC)E_2. However, the refinement of crystals structures of **3** and **7a** considering a *NCB* system produced better solution to the data set (with smaller *R* and *wR* values) than for the *CNB* isomer. Furthermore, on inspection of the parameters for the thermal ellipsoids, it has been observed that the sizes of the ellipsoids are consistent for the *NCB* systems, without any large discrepancies, unlike the case of the *CNB* systems. The X-ray diffraction data, correlated with the observations from ^{11}B{^{1}H} NMR spectroscopy, strongly indicate that **3** and **7a** contain BCN units.

The asymmetric unit of **3** consists of one 18-crown-6 macrocycle containing potassium, one [NCB(C_6F_5)$_3$]$^-$ anion unit and one molecule of toluene in a general position. Also present in the asymmetric unit is half a molecule of toluene disordered about an inversion centre. The asymmetric unit of **7a** contains only [Fe{(μ-NC)B(C_6F_5)$_3$}(η-C_5H_5)(CO)$_2$]. Figs. 3 and 4 show the ORTEP diagrams of the compounds [K(18-crown-6)][NCB(C_6F_5)$_3$] (**2**) and [Fe{(μ-NC)B(C_6F_5)$_3$}(η-C_5H_5)(CO)$_2$] (**7a**), respectively. The geometry around the boron centre is distorted tetrahedral in **3** and **7a**. For **3**, the C(1)–N(1) distance is 1.113(4) Å, whereas in **7a**, upon coordination to the Fe(II) centre, the corresponding distance increases to 1.135(3) Å. Both distances are slightly shorter than that found for [Zr{(μ-NC)-

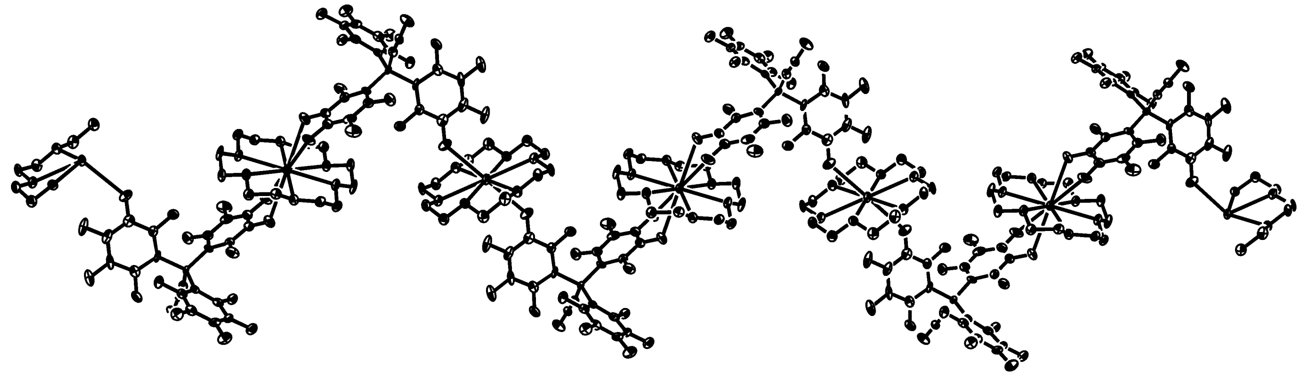

Fig. 2 Extended chain-like structure of [K(18-crown-6)][SCNB(C_6F_5)$_3$] (**1**).

Table 3 Selected bond lengths (Å) and angles (°) for compounds **1**, **3** and **7a**

1	C(1)–N(1)	1.180(3)	N(1)–C(1)–S(1)	178.3(2)
	C(1)–S(1)	1.598(2)	C(1)–N(1)–B(1)	173.1(2)
	C(11)–B(1)	1.650(3)	C(11)–B(1)–C(21)	112.12(16)
	C(21)–B(1)	1.654(3)	C(11)–B(1)–C(31)	112.02(16)
	C(31)–B(1)	1.647(3)	C(21)–B(1)–C(31)	112.86(19)
	N(1)–B(1)	1.531(3)	C(11)–B(1)–N(1)	106.03(18)
	K(2)–F(25)	2.8902(13)	C(21)–B(1)–N(1)	106.35(16)
	K(2)–O(53)	2.8024(13)	C(31)–B(1)–N(1)	106.89(17)
	K(2)–O(56)	2.8039(13)		
	K(2)–O(59)	2.7855(13)		
3	N(1)–C(1)	1.113(4)	N(1)–C(1) –B(1)	173.7(3)
	C(1)–B(1)	1.609(4)	C(1)–B(1)–C(11)	111.3(2)
	C(11)–B(1)	1.637(4)	C(1)–B(1)–C(21)	104.2(2)
	C(21)–B(1)	1.655(4)	C(11)–B(1)–C(21)	108.3(2)
	C(31)–B(1)	1.649(4)	C(1)–B(1)–C(31)	105.0(2)
	K(1)–N(1)	2.9189(14)	C(11)–B(1)–C(31)	113.0(2)
	K(1)–O(53)	2.9064(14)	C(21)–B(1)–C(31)	114.7(2)
	K(1)–O(56)	2.8387(14)	K(1)–N(1)–C(1)	121.60(11)
	K(1)–O(41)	2.8094(14)		
	K(1)–O(44)	2.8709(14)		
	K(1)–O(47)	2.7734(14)		
	K(1)–O(50)	2.8431(14)		
7a	Fe(1)–N(2)	1.9198(18)	Fe(1)–N(2)–C(3)	178.11(17)
	Fe(1)–C(38)	1.809(2)	N(2)–C(3)–B(4)	174.9(2)
	Fe(1)–C(40)	1.793(2)	C(3)–B(4)–C(5)	111.55(16)
	Fe(1)–C(42)	2.097(2)	C(3)–B(4)–C(16)	105.08(15)
	Fe(1)–C(43)	2.078(2)	C(5)–B(4)–C(16)	107.28(15)
	Fe(1)–C(44)	2.064(2)	C(3)–B(4)–C(27)	103.97(15)
	Fe(1)–C(45)	2.103(2)	C(5)–B(4)–C(27)	113.94(15)
	Fe(1)–C(46)	2.117(2)	C(16)–B(4)–C(27)	114.71(15)
	N(2)–C(3)	1.135(3)	Fe(1)–C(38)–O(39)	179.7(2)
	B(4)–C(3)	1.614(3)	Fe(1)–C(40)–O(41)	177.2(3)
	B(4)–C(5)	1.636(3)		
	B(4)–C(16)	1.653(3)		
	B(4)–C(27)	1.646(3)		
	C(38)–O(39)	1.127(3)		
	C(40)–O(41)	1.122(3)		

B(C_6F_5)$_3$}Me(Cp″)$_2$], where Cp″ = η-1,3-C_5H_3(SiMe$_3$)$_2$ (1.149(3) Å).[2] The C–B distances for **3** and **7a** were found to be 1.609(4) and 1.614(3) Å, respectively, close to the distance found for C–B in [Zr{(μ-NC)B(C_6F_5)$_3$}Me(Cp″)$_2$] (1.614(4) Å).[2] For both compounds, the B–C–N angles are approaching linearity (174.9(2)° in **7a** and 173.7(3)° in **3**) The C(1)–N(1)–K(1) angle found for **3** was 121.60(11)°, whereas the C–N–Fe unit of **7a** is almost linear (178.11(17)°). The latter is close to the angle C–N–Zr in [Zr{(μ-NC)B(C_6F_5)$_3$}Me(Cp″)$_2$], Cp″ = η-1,3-C_5H_3(SiMe$_3$)$_2$, which is 175.1(2)°.[2]

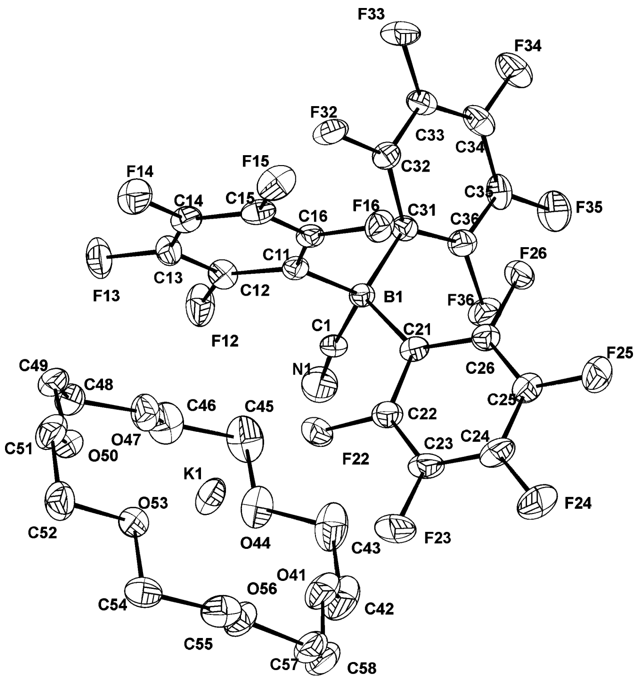

Fig. 3 ORTEP of [K(18-crown-6)][NCB(C_6F_5)$_3$] (**3**).

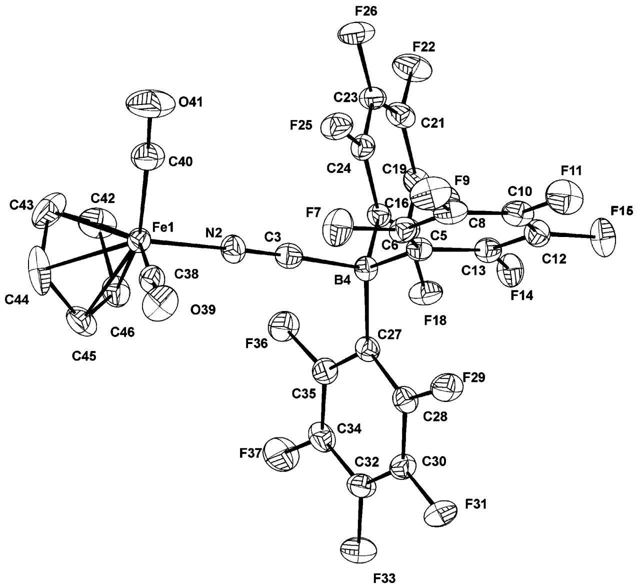

Fig. 4 ORTEP of [Fe{(μ-NC)B(C_6F_5)$_3$}(η-C_5H_5)(CO)$_2$] (**7a**).

DFT calculations

Density functional calculations have been carried out to investigate the relative stability of the system E$_1$(μ-NC)B *vs.* E$_1$(μ-CN)B for several of the new compounds. The C_6F_5 groups were substituted by fluorine atoms to reduce computational time. Geometry optimisations were carried out for the neutral species: [Me$_3$Si(μ-NC)BF$_3$] (**I**), [Me$_3$Si(μ-CN)BF$_3$] (**I′**), [Hg{(μ-NC)BF$_3$}$_2$] (**II**), [Hg{(μ-CN)BF$_3$}$_2$] (**II′**), [Fe{(μ-NC)BF$_3$}(η-C_5H_5)(CO)$_2$] (**III**), [Fe{(μ-CN)BF$_3$}(η-C_5H_5)(CO)$_2$] (**III′**) and for the anionic species [NCBF$_3$]$^-$ (**IV**), [CNBF$_3$]$^-$

Table 4 Crystallographic data for compounds **1**, **3** and **7a**

	1	**3**	**7a**
Chemical formula	$C_{31}H_{24}NBF_{15}KO_6S$	$C_{31}H_{24}NBF_{15}KO_6{\cdot}C_{10.5}H_{12}$	$C_{26}H_5NBF_{15}FeO_2$
Formula weight	873.47	979.62	714.97
Crystal system	Monoclinic	Triclinic	Triclinic
Space group	$P2_1/c$	$P\bar{1}$	$P\bar{1}$
Unit cell dimensions:			
a/Å	8.9130(5)	12.8240(5)	9.9080(4)
b/Å	21.0570(15)	12.9440(6)	10.4020(4)
c/Å	18.7380(14)	13.6630(6)	12.6890(6)
α/°	90	108.484(2)	97.594(2)
β/°	97.339(5)	98.684(2)	92.383(2)
γ/°	90	90.807(2)	99.853(2)
V/Å^3	3488.0	2121.7	1274.4
Z	4	2	2
D_c/g cm^{-3}	1.66	1.533	1.86
T/K	150	150	150
μ/mm^{-1}	0.34	0.240	0.73
Reflections collected	35534	17785	7026
Independent reflections	6629	8022	4866
R_{int}	0.04	0.018	0.03
Final R indices:			
R	0.0884	0.0828	0.0443
wR	0.0152	0.0712	0.0409

Note: criterion for observation, $I > 3\sigma(I)$.

(**IV′**) and $[F_3BNCBF_3]^-$ (**V**). Optimisations have also been performed on the model precursors Me_3SiCN, Me_3SiNC, $Hg(NC)_2$, $Hg(CN)_2$, $[Fe(NC)(\eta^5\text{-}C_5H_5)(CO)_2]$ and $[Fe(CN)(\eta\text{-}C_5H_5)(CO)_2]$. The results of all geometry optimisations are given in Table 5 together with the experimental values for compounds $[(C_6F_5)_3B(\mu\text{-}NC)B(C_6F_5)_3]$,[1,2] **7a** and **3**. All E_1–N–C–B and E_1–C–N–B systems are very close to linear. Reasonable agreement between calculated and experimental distances confirms that, in general, the model works well despite the replacement of the C_6F_5 groups with fluorine atoms. In general the N–C(B) distances are shorter than the C–N(B) ones. In both systems the C–N distances decrease very slightly on coordination by BF_3. The N–B distances for the $E_1(\mu\text{-}CN)B$ unit and the C–B distances for the $E_1(\mu\text{-}NC)B$ unit show significant variation in the order E_1 = Hg > Me_3Si > Fp > BF_3 > anion for both series. The B–F distances correlate inversely with the B–N and B–C distances.

Energies for the model compounds were calculated using both the local density approximation (LDA) and using gradient corrections (GGA). Table 6 gives the calculated isomerisation energy for both the parent nitriles and isonitriles and the $E_1(\mu\text{-}CN)B$ *vs.* $E_1(\mu\text{-}NC)B$ systems. Both methods give a similar pattern. The almost universal preference is for the isomer ($E_1(\mu\text{-}CN)B$).

Isomerisation between simple nitriles and isonitriles has been investigated both experimentally and computationally.[15,17,18] The general conclusions are that σ-accepting substituents favour nitriles (E_1CN) over isonitriles (E_1NC) and that π-accepting substituents favour isonitriles (E_1NC) over nitriles (E_1CN).[17] Our results are in agreement with this. In particular they agree with the low energy preference found for silylnitriles Si–CN where both σ- and π-accepting effects are important. For example values ranging between 18 and 31 kJ mol^{-1} have been calculated for the isomerisation energy of H_3Si–CN to H_3Si–NC using DFT.[18b]

The orbital responsible for the basic properties of the cyanide ion is the HOMO, 5σ (Fig. 5). This has electron density on both the C and the N but is more localised on C. Thus the C is generally the preferred basic atom in coordination to a Lewis acid. As it is primarily non-bonding in character, little change in CN distance results from coordination to a Lewis acid. Table 5 lists the Mulliken charges of C in the E_1NC systems and of N in the E_1CN systems. In the parent E_1–NC and E_1–CN molecules they are reduced compared with free cyanide, and further reduced on coordination to BF_3. Within a series the charge varies Hg < $SiMe_3$ < Fp < anion (the anion having the most negative charge). This correlates well with the C–B and N–B distances noted above, the least charged atoms forming the longer bonds to BF_3. Thus the better E_1 as a σ acceptor, the weaker the further bond for E_2–BF_3. From Table 6 it can be seen that the isomerisation energies are less favourable after BF_3 coordination. Just as nitriles E_1CN are generally found to be more stable than isonitriles E_1NC because C is the more basic site, the $E_1(\mu\text{-}NC)B$ systems are relatively more stabilised on BF_3 coordination as in this case it is the C atom that binds to the BF_3 group. The isomerisation energy difference for E_1= $SiMe_3$ is just sufficient to reverse the preference so that $[Me_3Si(\mu\text{-}NC)BF_3]$ is found to be marginally more stable than $[Me_3Si(\mu\text{-}CN)BF_3]$. Since Me_3SiNC and Me_3SiCN are known to be in equilibrium at room temperature, it is not surprising that treatment of Me_3SiCN with $B(C_6F_5)_3$ leads to formation of $[Me_3Si(\mu\text{-}NC)B(C_6F_5)_3]$ (**4**). In all other cases the calculations indicate the complexes $E_1(\mu\text{-}CN)B$ to be the thermodynamically favoured isomer.

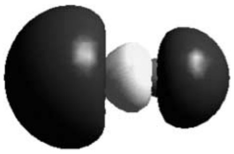

Fig. 5 The 5σ orbital of CN^-.

Conclusions

New main group and transition element derivatives of the anions $[SCNB(C_6F_5)_3]^-$, $[CNB(C_6F_5)_3]^-$ and $[NCB(C_6F_5)_3]^-$ have been prepared and characterised. New routes towards formation of complexes containing the bulky anionic ligand $[NCB(C_6F_5)_3]^-$ are described. We have observed formation of the $E_1(\mu\text{-}NC)B(C_6F_5)_3$ linkages in the complexes **6** and **7a**. Calculations indicate that in general energetic preference is for the $E_1(\mu\text{-}CN)B$.

Experimental

All reactions were carried out under dinitrogen, either in a glove-box or using conventional Schlenk-line techniques. The compounds $[FeCl(\eta\text{-}C_5H_5)(CO)_2]$,[19] $[Fe(CN)(\eta\text{-}C_5H_5)(CO)_2]$,[19]

Table 5 Selected DFT calculated distances (Å) and angles (°) for **I**–**V**, **I′**-**IV′**, Me_3SiCN, Me_3SiNC, FpCN, FpNC, $Hg(NC)_2$ and $Hg(CN)_2$. Where available experimental distances of the related $B(C_6F_5)_3$ derivatives are given for comparison (Fp = $Fe(\eta\text{-}C_5H_5)(CO)_2$)

Type *E₁NC*	E_1–N	N–C	C–B	B–F	Charge on C
I $[Me_3Si(\mu\text{-}NC)BF_3]$[a]	1.793	1.160	1.683	1.365	0.08
Me_3SiNC	1.760	1.178	–	–	−0.11
II $[Hg\{(\mu\text{-}NC)BF_3\}_2]$	1.935	1.162	1.712	1.361	0.03
$Hg(NC)_2$	1.94	1.177	–	–	−0.09
III $[Fp(\mu\text{-}NC)BF_3]$	1.860	1.158	1.655	1.372	−0.07
7a[b]	1.9198(18)	1.135(3)	1.614(3)	–	
FpNC	1.882	1.175	–	–	−0.19
IV $[NCBF_3]^-$	–	1.161	1.621	1.391	−0.07
3[c]	–	1.113(4)	1.609(4)	–	
$[CN]^-$		1.174			−0.5
V $[BF_3(\mu\text{-}NC)BF_3]^-$	1.578	1.152	1.644	1.379	0.07
$[(\mu\text{-}NC)\{B(C_6F_5)_3\}_2]^-$ [d]	–	1.144(2)	1.583(2)	–	
Type *E₁CN*	E_1–C	C–N	N–B	B–F	Charge on N
I′ $[Me_3Si(\mu\text{-}CN)BF_3]$[a]	1.885	1.152	1.643	1.353	−0.08
Me_3SiCN	1.885	1.161	–	–	−0.22
II′ $[Hg\{(\mu\text{-}CN)BF_3\}_2]$	1.986	1.150	1.752	1.350	0.03
$Hg(CN)_2$	1.989	1.160	–	–	−0.19
III′ $[Fp(\mu\text{-}CN)BF_3]$	1.828	1.158	1.596	1.367	−0.13
FpCN	1.872	1.165	–	–	−0.30
IV′ $[CNBF_3]^-$	–	1.168	1.537	1.386	−0.20
$[CN]^-$		1.174			−0.5
V $[BF_3(\mu\text{-}CN)BF_3]^-$	1.644	1.152	1.578	1.379	−0.2
$[(\mu\text{-}CN)\{B(C_6F_5)_3\}_2]^-$ [d]	–	1.144(2)	1.593(2)	–	

Note: [a] Average distances (Å) for Si–C(Me): 1.845 (**I**) and 1.850 (**I′**). [b] Average distances (Å): Fe–C(Cp) 2.070 (**II′**), 2.074 (**II**); Fe–C(O): 1.743 (**II**), 1.739 (**II′**), C–O 1.148 (**II**) and 1.147 (**II′**). [c] X-Ray values, this work. [d] X-Ray values, literature data.[1,2]

Table 6 Calculated energies ΔE_{isom} (kJ mol^{-1}) for the isonitrile (E_1–NC and $E_1(\mu\text{-}NC)B$) ⟶ nitrile (E_1–CN and $E_1(\mu\text{-}CN)B$) isomerisation energies at both the LDA and the GGA level

Isomerisation		ΔE_{isom}/kJ mol^{-1} (GGA)	ΔE_{isom}/kJ mol^{-1} (LDA)
$[Me_3Si(\mu\text{-}NC)BF_3] \longrightarrow [Me_3Si(\mu\text{-}CN)BF_3]$	**I**⟶**I′**	+3	+2
$Me_3SiNC \longrightarrow Me_3SiCN$		−20	−18
$[Hg\{(\mu\text{-}NC)BF_3\}_2] \longrightarrow [Hg\{(\mu\text{-}CN)BF_3\}_2]$	**II**⟶**II′**	−96	−102
$[Hg(NC)_2] \longrightarrow [Hg(CN)_2]$		−149	−153
$[Fp(\mu\text{-}NC)BF_3] \longrightarrow [Fp(\mu\text{-}CN)BF_3]$	**III**⟶**III′**	−60	−73
$[FpNC] \longrightarrow [FpCN]$		−79	−87
$[NCBF_3]^- \longrightarrow [CNBF_3]^-$	**IV**⟶**IV′**	+24	+20

and $B(C_6F_5)_3$,[20] were prepared according to the literature methods. $[IrCl(PPh_3)_2(CO)]$ was used as supplied by Aldrich. The compound $B(C_6F_5)_3$ was freshly sublimed before use. NMR spectra were recorded on either a 300 MHz Varian Mercury or a 500 MHz Varian Unity spectrometer, referenced internally using the residual protio-solvent, and chemical shifts were reported with respect to $SiMe_4$ (^1H and ^{13}C, $\delta = 0$), $BF_3{\cdot}Et_2O$ (^{11}B, $\delta = 0$), H_3PO_4 (^{31}P, $\delta = 0$) and $CFCl_3$ (^{19}F, $\delta = 0$). All chemical shifts are quoted in δ (ppm) and coupling constants in Hz. Infrared spectra were recorded on either a Perkin-Elmer 1710 IR FT spectrometer or a Perkin-Elmer 1600 FTIR. Elemental analyses and mass spectra were provided by the Microanalytical Services of the Inorganic Chemistry Laboratory, Oxford.

Preparations

[K(18-crown-6)][SCNB(C₆F₅)₃] (1). In a glove-box, a Schlenk vessel was charged with KSCN (38 mg, 0.39 mmol), $B(C_6F_5)_3$ (200 mg, 0.39 mmol). A separate Schlenk vessel was charged with 18-crown-6 ether (103 mg, 0.39 mmol) and 50 mL of toluene was added. This solution was added slowly under stirring to the Schlenk vessel containing a mixture of KSCN and $B(C_6F_5)_3$. The mixture was stirred at room temperature for 5 days. Volatiles were removed under reduced pressure to yield an off-white oily material, which was washed with 20 mL cold pentane. The resulting powder (crude yield: 254 mg, 74.5%) was recrystallised from a mixture of CH_2Cl_2 and pentane to give white crystals of **1**. The reaction was subsequently repeated in benzene, THF or CH_2Cl_2 and similar results were obtained.

Elemental analysis (%). Calc. (found) for $C_{31}H_{24}NBF_{15}KO_6S$: C 42.6 (42.3), H 2.8 (2.9), N 1.6 (1.5). FAB$^+$ *m/z* (intensity (%)): 873.2 (100) $[SCNB(C_6F_5)_3]^-$.

[K(18-crown-6)][(C₆F₅)₃B(μ-CN)B(C₆F₅)₃] (2). *Method 1.* In a glove-box, a Schlenk vessel was charged with KCN (25 mg, 0.38 mmol), $B(C_6F_5)_3$ (200 mg, 0.39 mmol). A separate Schlenk vessel was charged with 103 mg (0.391 mmol) 18-crown-6 ether and toluene (50 mL) was added and the resulting solution was added slowly to the initial mixture. This was then stirred at room temperature for 24 h and the solution turned orange. The white solid formed was isolated by filtration and dried under reduced pressure. ^1H- and $^{11}B\{^1H\}$-NMR spectra showed that this solid contains mainly starting materials. From the filtrate, volatiles were removed under reduced pressure to yield a brown oil. Recrystallisation from CH_2Cl_2 gave a small amount of light-yellow crystals (yield <10%) characterised by $^{11}B\{^1H\}$ NMR as $[K(18\text{-crown-}6)][(C_6F_5)_3B(\mu\text{-}CN)B(C_6F_5)_3]$ (**2**). The reaction was subsequently repeated in a number of different solvents (THF, toluene, CH_2Cl_2 or CH_3CN) using 2 : 2 : 1 or 1 : 1 : 2 ratios of 18-crown-6 ether, KCN and $B(C_6F_5)_3$. In each case, only the compound $[K(18\text{-crown-}6)][(C_6F_5)_3B(\mu\text{-}CN)B(C_6F_5)_3]$ (**2**) was obtained in low yield.

Method 2. In a glove-box, a Schlenk vessel was charged with 18-crown-6 ether (1 g, 3.8 mmol) and KCN (247 mg, 3.8 mmol). Dry methanol was then added, and the mixture was stirred at 40 °C overnight. The solution was then cooled to room temperature and the MeOH removed under reduced pressure. The residual white solid, was soluble in CH_2Cl_2 and insoluble in toluene and was washed with pentane and dried under reduced pressure to yield 1.16 g (93% yield) of [K(18-crown-6)CN]. Then $B(C_6F_5)_3$ in CH_2Cl_2 (50 mL) was added slowly to a solution of [K(18-crown-6)CN] (300 mg, 0.91 mmol) in 20 mL CH_2Cl_2. The mixture was stirred at room temperature under N_2 for 30 min. The volatiles were removed from the light-yellow solution under reduced pressure to give a creamy-white solid. This was extracted with toluene (10 mL). The toluene was removed under reduced pressure and the resulting brown, oily solid was recrystallised from a mixture of CH_2Cl_2 and pentane to give light-yellow crystals of [K(18-crown-6)][$(C_6F_5)_3B(\mu\text{-CN})B(C_6F_5)_3$] (**2**). Yield: 540 mg, 36%.

Elemental analysis (%). Calc. (found) for $C_{13}H_{24}NKO_6$: C 47.4 (47.7), H 7.3 (7.2), N 4.25 (4.3). Calc. (found) for $C_{49}H_{24}NB_2F_{30}KO_6$: C 43.5 (43.27), H 1.8 (1.9), N 1.0 (1.0). ES^- *m*/*z* (intensity (%)): 1046.28 (30) $[(C_6F_5)_3B(\mu\text{-CN})B(C_6F_5)_3]^-$.

[K(18-crown-6)][NCB(C_6F_5)$_3$] (3). *Method 1.* In a glove-box, a two-neck, round bottom flask was charged with potassium metal (230 mg, 5.88 mmol), [Hg{(μ-CN)B(C_6F_5)$_3$}$_2$] (**5**) (1 g, 0.783 mmol) (prepared as described below) and 18-crown-6 ether (415 mg, 1.57 mmol). Toluene (200 mL) was added and the mixture was stirred at the room temperature for 1 h. The mixture became cloudy, and was then heated at 90 °C for 7 h. The resulting black solid was removed by filtration. From the light-yellow filtrate, volatiles were removed under reduced pressure to yield an off-white solid. Recrystallisation from toluene at −80 °C gave the compound [K(18-crown-6)][NC{B(C_6F_5)$_3$}$_2$] (**3**) (450 mg, 29% yield) as colourless needle-like crystals.

Method 2. A solution of 18-crown-6 ether (140 mg, 0.53 mmol) in toluene (50 mL) was added to KCl (140 mg, 1.88 mmol) and the resulting mixture was stirred for 2 h. at room temperature. A solution of [$Me_3Si(\mu\text{-NC})B(C_6F_5)_3$] (**4**) (0.31 g, 0.53 mmol) (prepared as described below) in toluene (50 mL) was subsequently added and the mixture stirred for 2 h. The solids were removed by filtration and, from the filtrate, volatiles were removed under reduced pressure to give a white solid. After recrystallisation from toluene at −80 °C, 323 mg (73% yield) of compound **3** were obtained as fine colourless crystals, suitable for study by X-ray diffraction.

Elemental analysis (%). Calc. (found) for $C_{31}H_{24}NBF_{15}KO_6$: C 44.25 (44.0), H 2.8 (2.85), N 1.7 (1.7). ES^- *m*/*z* (intensity (%)): 536.09 (100) $[CN\{B(C_6F_5)_3\}_2]^-$.

[$Me_3Si(\mu\text{-NC})B(C_6F_5)_3$] (4). *NMR-scale reaction.* The compounds Me_3SiCN (0.013 mL, 0.1 mmol) and $B(C_6F_5)_3$ (0.05 g, 0.1 mmol) were mixed at room temperature in a glove-box in a Young's tap NMR tube and C_6D_6 was added. The NMR spectra, recorded within 15 min, showed quantitative formation of [$Me_3Si(\mu\text{-NC})B(C_6F_5)_3$] (**4**). *Synthesis.* Me_3SiCN (0.15 mL, 1.12 mmol) in 40 mL CH_2Cl_2 was added to $B(C_6F_5)_3$ (0.6 g, 1.17 mmol) in 20 mL CH_2Cl_2 and the resulting mixture was subsequently stirred for 1 h. The solvents were removed under reduced pressure, the crude yellow–white powder was washed with pentane (2 × 15 mL), and the product was recrystallised from a saturated CH_2Cl_2 solution layered with pentane. Compound **4** (530 mg, 77% yield) was isolated as a white, micro-crystalline material.

Elemental analysis (%). Calc. (found) for $C_{22}H_9NBF_{15}Si$: C 43.2 (42.9), H 1.5 (1.1), N 2.3 (2.0). FAB^+ *m*/*z* (intensity (%)): 610.2 (40) $[Me_3SiNCB(C_6F_5)_3]^+$.

[Hg{(μ-CN)B(C_6F_5)$_3$}$_2$] (5). In a glove-box, the compounds [$Hg(CN)_2$] (0.25 g, 0.97 mmol) and $B(C_6F_5)_3$ (1 g, 1.95 mmol) were mixed in a Schlenk vessel and 50 mL CH_2Cl_2 added. The mixture was stirred at room temperature under N_2 for 15 h. From the clear solution, the volatiles were removed under reduced pressure to give a white solid, which was washed with pentane (2 × 10 mL) and dried under reduced pressure to give 1.1 g (87% yield) **5** as a white solid.

Elemental analysis (%). Calc. (found) for $C_{38}N_2F_{30}B_2Hg$: C 35.75 (36.0), N 2.2 (2.3). FAB^+ *m*/*z* (intensity (%)): 1277.6 (85) $[Hg\{(\mu\text{-CN})B(C_6F_5)_3\}_2]^+$.

[Ir{(μ-NC)B(C_6F_5)$_3$}(PPh_3)$_2$(CO)] (6). [$Me_3Si(\mu\text{-NC})B(C_6F_5)_3$] (**4**) was prepared *in situ* by addition of Me_3SiCN (0.033 mL, 0.25 mmol) to a solution of $B(C_6F_5)_3$ (128 mg, 0.25 mmol) in CH_2Cl_2 (50 mL). The mixture was then stirred for 5–10 min before being added to a solution of [$IrCl(PPh_3)_2(CO)$] (195 mg, 0.25 mmol) in CH_2Cl_2 (50 mL). The solution was left stirring for 2 h, and the initially pale yellow colour changed to a bright-yellow. The solution was subsequently filtered, volatiles removed under reduced pressure and the resulting residue was washed with pentane (2 × 20 mL) to yield a yellow powder. The solid was then recrystallised from CH_2Cl_2 at −80 °C to give compound **5** (120 mg, 37% yield) as a microcrystalline yellow powder.

Elemental analysis (%). Calc. (found) for $C_{56}H_{30}NOBF_{15}IrP$: C 52.4 (52.2), H 1.1 (1.2), N 2.4 (2.65). FAB^+ *m*/*z* (intensity (%)): 1282.5 (8.5) $[Ir\{(\mu\text{-NC})B(C_6F_5)_3\}(PPh_3)_2(CO)]^+$.

[Fe{(μ-NC)B(C_6F_5)$_3$}(η-C_5H_5)(CO)$_2$] (7a). [$Me_3Si(\mu\text{-NC})B(C_6F_5)_3$] (**4**) was prepared *in situ* by addition of Me_3SiCN (0.13 mL, 1.00 mmol) to a solution of $B(C_6F_5)_3$ (512 mg, 1.00 mmol) in CH_2Cl_2 (50 mL). The mixture was then stirred for 30 min before being added to a solution of [$Fe(\eta\text{-}C_5H_5)(CO)_2Cl$] (213 mg, 1.00 mmol) in CH_2Cl_2 (50 mL). The solution was then left stirring overnight, after which time the red colour had darkened to red–brown. The volatiles were subsequently removed under reduced pressure to a red solid. This was washed with light petroleum (bp 40–60 °C) (2 × 15 mL) and recrystallised from a 1 : 1 mixture of pentane and CH_2Cl_2 to give 486 mg (68% yield) of **7a** as a red, microcrystalline solid. Crystals of **7a**, suitable or for X-ray analysis were obtained by diffusion of pentane into a concentrated CH_2Cl_2 solution.

Elemental analysis (%). Calc.(found) for $C_{26}H_5NBF_{15}FeNO_2$: C 43.7 (43.2), H 0.7 (0.3) N 2.00 (1.8) Fe 7.8 (7.1). FAB^+ *m*/*z* (intensity (%)): 715.0(5) $[Fe\{NCB(C_6F_5)_3\}(C_5H_5)(CO)_2]^+$, 658.9(13.5) $[Fe\{(\mu\text{-NC})B(C_6F_5)_3\}(\eta\text{-}C_5H_5)]^+$.

[Fe(μ-CN)B(C_6F_5)$_3$(η-C_5H_5)(CO)$_2$} (7b). The solids $B(C_6F_5)_3$ (20 mg, 0.039 mmol) and [$Fe(CN)(\eta^5\text{-}C_5H_5)(CO)_2$] (5 mg, 0.025 mmol) were placed in a Young's tap NMR tube and C_6D_6 (or CD_2Cl_2) added. ^1H-, ^{19}F- and $^{11}B\{^1H\}$-NMR spectra recorded within 15 min showed the quantitative formation of [$Fe\{(\mu\text{-CN})B(C_6F_5)_3\}(\eta\text{-}C_5H_5)(CO)_2$] (**7b**).

X-Ray crystallography

In each case, a single crystal was selected under an inert atmosphere, encased in perfluoro-polyether oil, and mounted on the end of a glass fibre. The fibre, secured in a goniometer head was then placed under a stream of cold nitrogen maintained at 150 K and data collected on an Enraf-Nonius DIP2000 image plate diffractometer with graphite monochromated Mo-Kα radiation (λ = 0.71069 Å) The images were processed with the DENZO and SCALEPACK programs[21] and corrections for Lorentz and polarisation effects were performed. All solution, refinement, and graphical calculations were performed using the CRYSTALS[22] and CAMERON[23] software packages. The structures were solved by direct methods using the SIR92[24] program and refined by full-matrix least squares procedure on *F*. All non-hydrogen atoms were refined with anisotropic displacement parameters. All hydrogen atoms were generated and allowed to ride on their corresponding carbon atoms with fixed thermal parameters. An empirical absorption correction was applied.[25] The crystallographic data are summarised in Table 3. In addition, refinement using full-matrix least squares on all F^2 data[26] was also performed for **3** and **7a**. Both refinements methods (either on F or on F^2) gave better results (lower R and wR) for the model with the CN group N-bound to the metal (K in case of **3**, or Fe in case of **7a**) than for the model where this group is C-bond to the metal. The inspection of the parameters for the thermal ellipsoids also indicated that the model containing *NCB* units are better solutions to the data sets than those incorporating the *CNB* units. These results are consistent with the observations from $^{11}B\{^{1}H\}$ NMR spectroscopy and the previously reported data.[2]

CCDC reference numbers 204648–204650.

See http://www.rsc.org/suppdata/dt/b3/b302163g/ for crystallographic data in CIF or other electronic format.

Computational details

All calculations were performed using density functional methods of the Amsterdam Density Functional Package (version 2000.2).[27–30] The electronic configurations of the molecular systems were described using type IV basis sets with triple ζ accuracy sets of Slater type orbitals, with a single polarisation function added to the main group atoms. The cores of the atoms were frozen up to 2p for Fe, 4d for Hg, 1s for C, O and N, 2p for Si. First-order relativistic corrections were made to the cores of all atoms using the ZORA formalism. The generalised gradient approximation (GGA non-local) method was used, using Vosko, Wilk and Nusair's local exchange correlation[31] with non-local exchange corrections by Becke[32] and non-local correlation corrections by Perdew.[33] The non-local correction terms were not utilised in calculating gradients during geometry optimisations as better agreement with experimental structure is normally achieved with a local density approximation.

Acknowledgements

We thank Dr Neale G. Jones for helpful discussions, Drs David J Watkin and Andrew R. Cowley for assistance with crystallography, Balliol College Oxford for a Dervorguilla Scholarship (S. I. P), the AG Leventis Foundation for a grant (to I.C.V) and EPSRC for support (to G. D. W. A.). Part of this work was carried out using the resources of the Oxford Super Computing Centre and part using the EPSRC Columbus cluster at the Rutherford Laboratory.

References

1 S. J. Lancaster, D. A. Walker, M. Thornton-Pett and M. Bochmann, *Chem. Commun.*, 1999, 1533.
2 J. Zhou, S. J. Lancaster, D. A. Walker, S. Beck, M. Thornton-Pett and M. Bochmann, *J. Am. Chem. Soc.*, 2001, **123**, 223.
3 A. A. Danopoulos, J. R. Galsworthy, M. L. H. Green, S. Cafferkey, L. H. Doerrer and M. B. Hursthouse, *Chem. Commun.*, 1998, 2529.
4 L. H. Doerrer, J. R. Galsworthy, M. L. H. Green, M. A. Leech and M. Mueller, *J. Chem. Soc., Dalton Trans.*, 1998, 3191.
5 L. H. Doerrer, J. R. Galsworthy, M. L. H. Green and M. A. Leech, *J. Chem. Soc., Dalton Trans.*, 1998, 2483.
6 L. H. Doerrer, A. J. Graham and M. L. H. Green, *J. Chem. Soc., Dalton Trans.*, 1998, 3941.
7 L. H. Doerrer and M. L. H. Green, *J. Chem. Soc., Dalton Trans.*, 1999, 4325.
8 J. L. Priego, L. H. Doerrer, L. H. Rees and M. L. H. Green, *Chem. Commun.*, 2000, 779.
9 H. Jacobsen, H. Berke, S. Doering, G. Kehr, G. Erker, R. Froehlich and O. Meyer, *Organometallics*, 1999, **18**, 1724.
10 L. Li and T. J. Marks, *Organometallics*, 1998, **17**, 3996.
11 C. Bergquist, B. M. Bridgewater, C. J. Harlan, J. R. Norton, R. A. Friesner and G. Parkin, *J. Am. Chem. Soc.*, 2000, **122**, 10581.
12 D. E. J. Arnold, S. Cradock, E. A. V. Ebsworth, J. D. Murdoch, D. W. H. Rankin, D. C. J. Skea, R. K. Harris and B. J. Kimber, *J. Chem. Soc., Dalton Trans.*, 1981, 1349.
13 W. R. Hertler, D. A. Dixon, E. W. Matthews, F. Davidson and F. G. Kitson, *J. Am. Chem. Soc.*, 1987, **109**, 6532.
14 K. Georgiou and A. C. Legon, *J. Mol. Struct.*, 1982, **78**, 257.
15 I. Ugi, *Isocyanide Chemistry*, Academic Press, New York, 1971.
16 G. Barrado, L. H. Doerrer, M. L. H. Green and M. A. Leech, *J. Chem. Soc., Dalton Trans.*, 1999, 1061.
17 H. Vahrenkamp, A. Geiss and G. N. Richardson, *J. Chem. Soc., Dalton Trans.*, 1997, 3643.
18 (*a*) K. Sung, *J. Org. Chem.*, 1999, **64**, 8984; (*b*) C. Zanchini, *Chem. Phys.*, 2000, **254**, 187.
19 T. S. Piper, F. A. Cotton and G. Wilkinson, *J. Inorg. Nucl. Chem.*, 1955, **1**, 165.
20 J. L. W. Pohlmann and F. E. Brinckmann, *Z. Naturforsch., Teil B*, 1965, **20**, 5.
21 Z. Otwinowski and W. Minor, *Methods Enzymol.*, 1996, 276.
22 D. J. Watkin, C. K. Prout, J. R. Carruthers and P. W. Betteridge, in *CRYSTALS*, Issue 10, Chemical Crystallography Laboratory, Oxford, 1996.
23 D. J. Watkin, C. K. Prout and L. J. Pearce, in *CAMERON*, Chemical Crystallography Laboratory, Oxford, 1996.
24 A. Altomare, G. Carascano, C. Giacovazzo and A. Guagliardi, *J. Appl. Crystallogr.*, 1993, **26**, 343.
25 N. Walker and D. Stuart, *Acta Crystallogr., Sect. A*, 1983, **39**, 158.
26 G. M. Sheldrick, in SHELXL93 - Program for Crystal Structure Refinement, Göttingen, 1993.
27 E. J. Baerends, E. G. Ellis and P. Ros, *Chem. Phys.*, 1973, **2**, 41.
28 C. Fonseca Guerra, J. G. Snijider, B. te Velde and E. J. Baerends, *Theor. Chem. Acc.*, 1998, **99**, 391.
29 B. te Velde and E. J. Baerends, *J. Comput. Phys.*, 1992, **99**, 84.
30 L. Verluis and T. Ziegler, *J. Chem. Phys.*, 1988, **88**, 322.
31 S. H. Vosko, L. Wilk and M. Nusair, *Can. J. Phys.*, 1990, **58**, 1200.
32 A. D. Becke, *Phys. Rev. A*, 1988, **38**, 2398.
33 J. Perdew, *Phys. Rev. B*, 1986, **33**, 8822.